Journal of Colloid and Interface Science 430 (2014) 326–336

Contents lists available at ScienceDirect

Journal of Colloid and Interface Science

www.elsevier.com/locate/jcis

Self-aggregation of cationic dimeric surfactants in water–ionic liquid binary mixtures

Victoria Isabel Martín [a], Amalia Rodríguez [a], André Laschewsky [b,c], María Luisa Moyá [a,*]

[a] Department of Physical Chemistry, University of Seville, Profesor García González 1, 41012 Seville, Spain
[b] Institut für Chemie, Universitat Postdam, Karl-Liebknecht Str. 25, 14476 Postdam-Golm, Germany
[c] Fraunhofer Institute of Applied Polymer Research, Geiselbergstr. 69, 14476 Postdam-Golm, Germany

ARTICLE INFO

Article history:
Received 23 April 2014
Accepted 31 May 2014
Available online 10 June 2014

In memory of Professor Amalia Rodríguez

Keywords:
Dimeric surfactants
Micellization
Micelle growth
Ionic liquids
Background electrolyte
Co-solvent
ROESY
Dynamic light scattering

ABSTRACT

The micellization of four dimeric cationic surfactants ("gemini surfactants") derived from N-dodecyl-N,N,N-trimethylammonium chloride was studied in pure water and in water–ionic liquid (IL) solutions by a wide range of techniques. The dimeric surfactants are distinguished by their rigid spacer groups separating the two surfactant motifs, which range from C_3 to C_5 in length. In order to minimize organic ion pairing effects as well as the role of the ionic liquids as potential co-surfactants, ILs with inorganic hydrophilic anions and organic cations of limited hydrophobicity were chosen, namely ethyl, butyl, and hexyl-3-imidazolium chlorides. ^{1}H NMR two-dimensional, 2D, rotating frame nuclear Overhauser effect spectroscopy measurements, ROESY, supported this premise. The spacer nature hardly affects the micellization process, neither in water nor in water–IL solutions. However, it does influence the tendency of the dimeric surfactants to form elongated micelles when surfactant concentration increases. In order to have a better understanding of the ternary water–IL surfactant systems, the micellization of the surfactants was also studied in aqueous NaCl solutions, in water–ethylene glycol and in water–formamide binary mixtures. The combined results show that the ionic liquids play a double role in the mixed systems, operating simultaneously as background electrolytes and as polar organic solvents. The IL role as organic co-solvent becomes more dominant when its concentration increases, and when the IL alkyl chain length augments.

1. Introduction

Dimeric surfactants are amphiphilic molecules that contain two hydrophobic tails and two head groups connected at the level of the head groups by a spacer that may be hydrophilic, hydrophobic, flexible or rigid [1,2]. Their structure confers them superior properties compared to the corresponding conventional (single-chain) surfactants. They have lower cmc, stronger efficiency in reducing the surface tension of water, better wetting power, better solubility power, better foaming, etc. [1–3]. All these advantages make them of special interest for biomedical and technological applications, where they have been investigated as drug delivery systems, DNA carriers, nanoreactors for enzymatic reactions, emulsifying agents, detergents, etc. [3–12].

The solution properties of surfactants can be modulated by controlling temperature, pressure and/or by addition of different modifiers (e.g. cosolvents, cosurfactants, electrolytes, etc.) [13,14]. Ionic liquids, ILs, are a class of organic electrolytes, which are composed of an organic cation and an inorganic or organic anion, that melt at temperature lower than 100 °C [15]. An advantage of ILs is that by combining organic cations with suitable anions it is possible to tailor their physical and chemical properties. In general ILs are considered environmentally friendly compounds because mostly they are non-flammable and non-volatile. Besides, many ILs have an excellent chemical and thermal stability, wide liquid temperature ranges and wide electrochemical windows. Therefore ILs have been widely used in organic synthesis, catalysis, nanomaterial separation, chemical separation, etc. [16–20]. For the application of ILs in such fields, they are frequently used with water, whose presence can strongly affect their physical and chemical properties of ILs [21–23]. The surfactant–water–IL three component systems are particularly interesting because ILs can behave not only as co-solvents, but also as background electrolytes and as co-surfactants, their main role depending on the IL structure [24–29]. This gives the opportunity of tuning the physicochemical properties of the surfactant aggregates formed

* Corresponding author. Fax: +34 954557174.
E-mail addresses: laschews@uni-potsdam.de (A. Laschewsky), moya@us.es (M.L. Moyá).

http://dx.doi.org/10.1016/j.jcis.2014.05.064
0021-9797/

in water–IL binary mixtures, which is of interest for potential applications. Bearing this in mind, we investigated the effects of the addition of ethyl-3-methylimidazolium chloride, C_2mimCl, butyl-3-methylimidazolium chloride, C_4mimCl, and hexyl-3-methylimidazolium chloride, C_6mimCl, on the aggregation of various cationic dimeric surfactants (see Scheme 1) in aqueous solutions at 303 K. Since the dimeric surfactants studied contain chloride as common counterion, ILs with the same anion were chosen, while the hydrophobic substituents on their organic cations were confined to short or medium alkyl chains in order to minimize their possible role as co-surfactants [30]. The dimeric surfactants investigated have all dodecyl hydrophobic chains, but different rigid spacers, namely two isomeric pairs of butylidene and xylidine moieties that separate the ammonium groups by three to five carbon atoms. Therefore, the results obtained in this work will give relevant information about the influence of the dimeric surfactant spacer nature, with respect to either its length for a given hydrophobicity, or to its hydrophobicity for a given length, on the micellization in water–IL solutions. The studies were also aimed at a deeper understanding of the role played by the ionic liquids on micellization, and of the dependence of this role on the IL alkyl chain length. The results will provide useful information on how to tune the physicochemical properties of the surfactant aggregates in aqueous solution by adding ILs.

Before studying the surfactants in water–IL solutions, the aqueous dimeric surfactants solutions were thoroughly characterized at 303 K. This characterization includes the study of changes in the size and shape of the micelles caused by an increase in surfactant concentration and their dependence on the dimeric surfactant spacer group.

2. Experimental

2.1. Materials

The dimeric surfactants were synthesized as described previously [31]. The ILs were from Fluka, of the highest purity available, and were used as received. Pyrene-3-carboxaldehyde, P3C, and NaCl were from Aldrich. Pyrene was from Aldrich and it was purified before use by methods reported in the literature [32]. N-Hexadecylpyridinium chloride (cetylpyridinium chloride, CpyCl), methyl 4-nitrobenzenesulfonate and dodecyltrimethylammonium chloride were purchased from Fluka. 6-Methoxy-N-(3-sulfopropyl)quinolinium, SPQ, was from Molecular Probes, Inc. and used as received.

All solutions were prepared in double-distilled water (resistivity >18 MΩ cm).

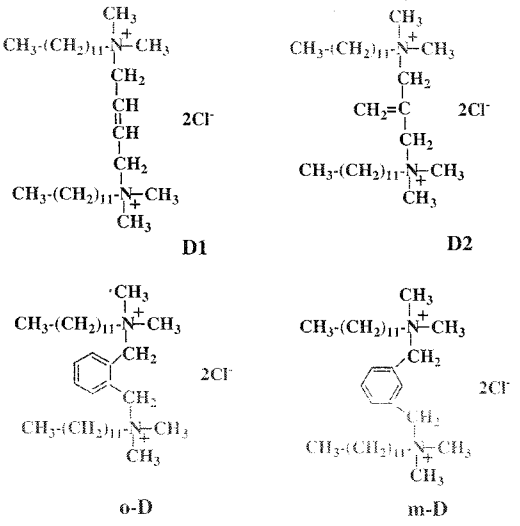

Scheme 1. Structure of the dimeric surfactants investigated in this work.

2.2. Conductivity measurements

Conductivity was measured with a Crison GLP31 conductimeter as described in Ref. [33].

2.3. Fluorescence measurements

Fluorescence measurements were performed by using a Hitachi F-2500 fluorescence spectrophotometer. The temperature was kept at 303 K by a water flow cryostat connected to the cell compartment.

2.3.1. cmc's determination by using pyrene as probe

The 1×10^{-6} M pyrene surfactant solutions were prepared as is described in Ref. [34]. The excitation wavelength was 335 nm and the fluorescence intensities were measured at 373 nm (band 1) and 384 nm (band 3). Excitation and emission slits were 2.5 nm and a scan speed of 60 nm/min was used. The intensity ratio of the vibronic bands (1:3) is called the pyrene 1:3 ratio [35].

2.3.2. Second critical micelle concentration, C″, determination

The SPQ concentration in the surfactant solutions was 1×10^{-6} M. The excitation wavelength was 346 nm and the fluorescence intensity was measured at 443 nm, as indicated in Ref. [36]. Excitation and emission slits were 5 and 10 nm, respectively, and a scan speed of 60 nm/s was used. Surfactant concentrations were well above the cmc.

2.3.3. Average micellar aggregation number determination

Pyrene (1×10^{-6} M) micellar solutions were prepared as in Ref. [34]. The fluorescence quenching of pyrene by cetylpyridinium chloride, CPyCl, was studied by exciting the pyrene at 335 nm, and recording its emission at 374 nm, with the use of excitation and emission slits of 2.5 and 2.5 nm, respectively. A scan speed of 60 nm/min was used. The low pyrene concentration avoided excimer formation, and the CpyCl concentration was varied in such a way that [pyrene]/[micelles] and [quencher]/[micelles] ratios were low enough to ensure a Poisson distribution [37,38].

2.3.4. Study of the polarity of the micellar interfacial region

The 10^{-5} M pyrene-3-carboxaldehyde, P3C, micellar solutions were prepared as in Ref. [34]. P3C was excited at 356 nm and fluorescence spectra were recorded from 380 to 600 nm. A scan speed of 60 nm/min was used and the excitation and emission slits were 5 nm and 10 nm, respectively. In order to check the reliability of our data, the fluorescence emission spectrum of P3C in a 0.1 M aqueous dodecyltrimethylammonium bromide, DTAB, micellar solution was recorded. The fluorescence maximum was 446 nm, in good agreement with literature data [35]. The precision in the measurements was ±1 nm.

2.4. Surface tension measurements

Surface tension was measured by a du Noüy ring method using a KSV 703 digital tensiometer (Finland) as described in Ref. [33]. The precision in the measurements was $\pm(1 \times 10^{-3})$ N m^{-1}. Care has to be taken in using the du Noüy ring method to deduce surfactant properties, because the surfactant adsorption kinetics can influence the results [39]. In our experiments the ring rising velocity was chosen low enough to allow the surfactant adsorption to

reach equilibrium. This was particularly important when surface tension of dimeric surfactant solutions was measured.

2.5. NMR measurements

The NMR spectra were performed in CITIUS (Research General Services for the University of Seville). NMR samples were prepared by dissolving the corresponding amount of the surfactant and the IL in D_2O followed by a brief sonication. NMR experiments were recorded on a Bruker Avance 500 spectrometer (500.2×10^6 Hz for ^1H) equipped with a 5 mm inverse probe and a Great 1/10 pulsed-gradient unit capable of producing magnetic field gradients in the z direction of about 50 G cm $^{-1}$. The chemical shifts in the ^1H NMR spectra were referenced to the residual HDO signal [40].

Two-dimensional, 2D, rotating frame nuclear Overhauser effect spectroscopy (ROESY) was performed at 500 MHz with the Bruker standard pulse sequences; the data consisted of 8 transients collected over 2049 complex points. A mixing time of 0.250 s, a repetition delay of 1.2 s, and a 90° pulse width of 11.0/s were used. The ROESY data set was processed by applying an exponential function in both dimensions and zero filling to 2048×2048 real data points prior to the Fourier transformation. All ROESY spectra were made symmetrical about the diagonal.

2.6. Kinetic measurements

The reaction between methyl 4-nitrobenzenesulfonate, MBS, and chloride ions (Scheme 2) was recorded at 280 by using a Hitachi 3100 UV–visible spectrophotometer as described in Ref. [41]. The temperature was maintained at 303.0 ± 0.1 K using a water-jacketed cell compartment connected to a water-flow cryostat. Each experiment was repeated at least twice, and the observed rate constants were reproducible within a precision better than 4%.

The reaction of the organic substrate with water can make a contribution to the process MBS + Cl^- [42], although this contribution is not significant except at low surfactant concentrations. Kinetic data have been corrected, when necessary, from the spontaneous hydrolysis contribution as in Ref. [41].

2.7. Dynamic light scattering, DLS, measurements

A Zetasizer Nano ZS (Malvern) was used for the measurement of hydrodynamic diameter (Z-average) at 303 K. The intensity of the scattered light was observed at 90°. The apparatus is in CITIUS. The surfactant concentration was fixed at 0.05 M and the IL concentration was changed. For this [surfactant] the quality of the signal was good and the standard deviation of the measurements remains low. Six measurements were made at each IL concentration and the average value was considered.

2.8. Atomic Force Microscopy (AFM)

The images were obtained with a Molecular Imaging PicoPlus 2500 AFM (Agilent Technologies). The apparatus is CITIUS. Cantilevers (Model PPP-FMR-20, Nanosensor) with a resonance frequency within 45–115 Hz were used. All AFM imaging was recorded in air and in tapping mode, with scan speeds of about 0.5 Hz and data collection at 256×256 pixels. AFM images were obtained by drying 30 μL droplet of the working solution, deposited on a freshly cleaved mica surface, adsorbed for 30 min, the surface washed with double distilled water, and then air-dried.

The experimental results were treated with the software WSxM 4.0 Beta 6.2 from Nanotec [43].

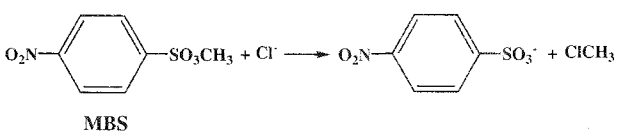

MBS

Scheme 2.

3. Results and discussion

3.1. Physicochemical characterization of the aqueous dimeric surfactants solutions

The critical micellar concentration, cmc, and the micellar ionization degree, α, were estimated by conductivity measurements (see Fig. 1). The dependence of the specific conductivity on surfactant concentration was fitted using Carpena's method [44], and the cmc and α values obtained are listed in Table 1.

The Gibbs energy of micellization, ΔG°_M, can be calculated by using Eq. (1) [45]:

$$\Delta G^\circ_M = 2RT(1.5 - \alpha)\ln(\text{cmc}) \quad (1)$$

where α is the micellar ionization degree, cmc is the critical micelle concentration expressed as mole fraction, and R and T have their usual meaning. The ΔG°_M values are also summarized in Table 1.

Table 1 shows that the cmc's of all the surfactants investigated are similar, within the experimental errors. This result can be explained by considering that the driving force for the self-association process of surfactants is the Gibbs energy contribution of the transfer of the hydrophobic surfactant tails from the aqueous phase into the micellar interior, ΔG°_{transf} [46]. Since all the surfactants have two dodecyl chains, ΔG°_{transf} is expected to be analogous for all of them and, therefore, the cmc is also expected to be similar, as observed. The estimated micellar ionization degrees are also nearly the same for all the surfactants, within the experimental error. As a consequence, similar ΔG°_M values are found for the four surfactants studied, thus pointing out that – within the variation made – the nature of the spacer does not practically influence the tendency of the surfactants to self-organize.

The micellization process was also studied by means of ^1H NMR measurements, extending some preliminary earlier experiments [31,33]. Two different surfactant concentrations were prepared, one below the cmc and one above the cmc. It was found that the chemical shift variations upon changing [surfactant] from below to above the cmc are more pronounced for the protons located closer to the ionic head groups of the surfactant, as is expected for a self-organization process [47].

In order to investigate the position of the spacers within the dimeric micelles, two-dimensional, 2D, rotating frame nuclear Overhauser effect spectroscopy (ROESY) experiments were carried out. Fig. 2 shows a partial ROESY spectrum of a solution containing 5×10^{-3} M of o-D at 303 K. Cross-peaks between the H-phenyl(1) and the protons belonging to the alkyl chain are observed. These peaks are due to the proximity of these protons in an o-D molecule. Similar cross-peaks were found for the surfactant m-D (Ref. [33] and Fig. 1S), indicating that the phenyl ring is buried toward the micelle interior, with the cationic ammonia groups protruding into the aqueous phase. Molecular dynamics, MD, simulations, carried out in collaboration with Dr. Luis J. Álvarez in order to elucidate the structural details of m-D and o-D molecules within the micelles, indicate that the phenyl rings are bent towards the hydrophobic micellar interior, in agreement with the experimental observations. ROESY spectra for the surfactants D1 and D2 do not show cross peaks.

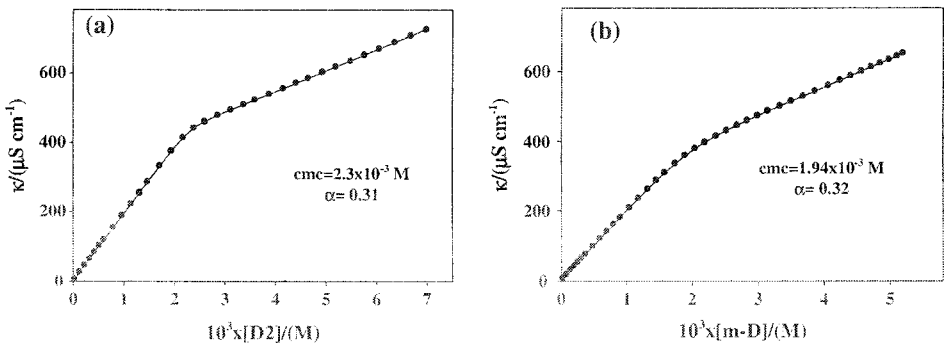

Fig. 1. Dependence of the specific conductivity, $\kappa/\mu S\ cm^{-1}$, on surfactant concentration: (a) D2 and (b) m-D. $T = 303$ K. The solid line corresponds to the Carpena fitting.

Table 1
Critical micelle concentration, cmc, micellar ionization degree, α, average aggregation number, N_{agg}, second critical micellar concentration, C^*, and Gibbs energy of micellization, ΔG^o_M, for the aqueous dimeric surfactant solutions studied at 303 K.

Surfactant	$10^3 \times$ cmc (M)	α	N_{agg}[a]	C^* (M)	ΔG^o_M (kJ mol^{-1})
D1	2.2 ± 0.1	0.35 ± 0.02	22 ± 2	0.067 ± 0.003	−59
D2	2.3 ± 0.1	0.31 ± 0.01	23 ± 2	0.051 ± 0.002	−61
o-D	2.03 ± 0.08	0.30 ± 0.02	22 ± 2	0.045 ± 0.002	−62
m-D	1.94 ± 0.07	0.32 ± 0.01	20 ± 1	0.052 ± 0.003	−61

[a] $[Surfactant_m] = 0.01$ M.

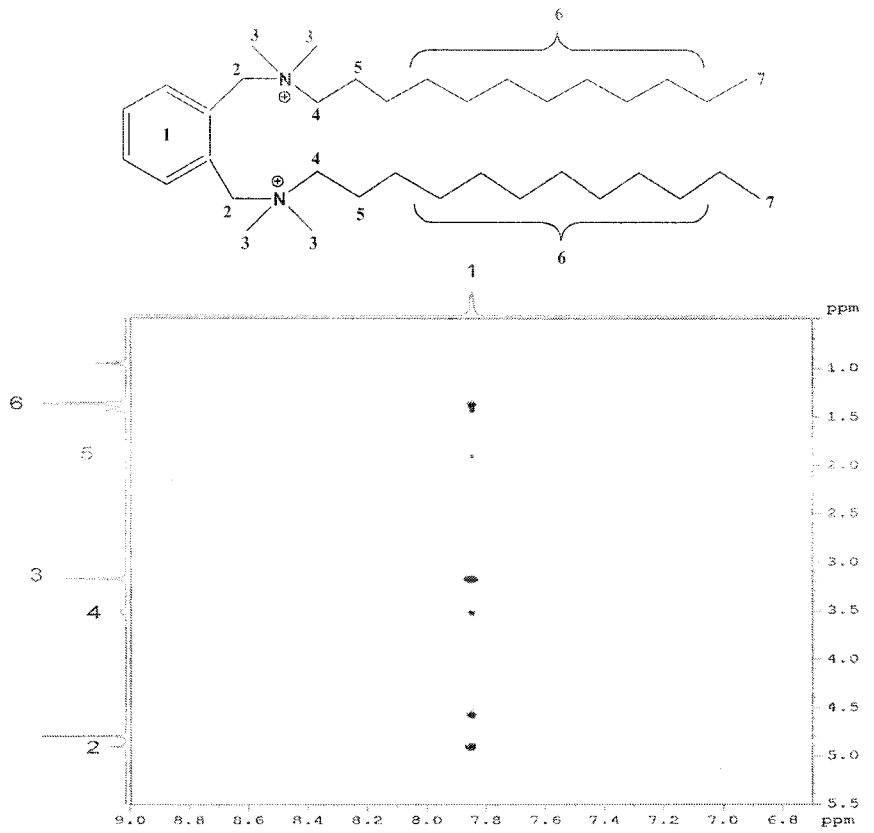

Fig. 2. Partial ROESY spectrum of an aqueous micellar solution of [o-D] = 5×10^{-3} M. $T = 303$ K.

The average micellar aggregation numbers of the micelles formed by the surfactants investigated in water, at a micellized surfactant concentration equal to 0.01 M, were obtained using the fluorescence quenching of pyrene by CpyCl (see Fig. 3). This surfactant concentration was chosen in order to make certain the micelles are spherical. It will be seen below that an increase in the surfactant concentration could result in the change of the shape and size of the aggregates present in the surfactant solu-

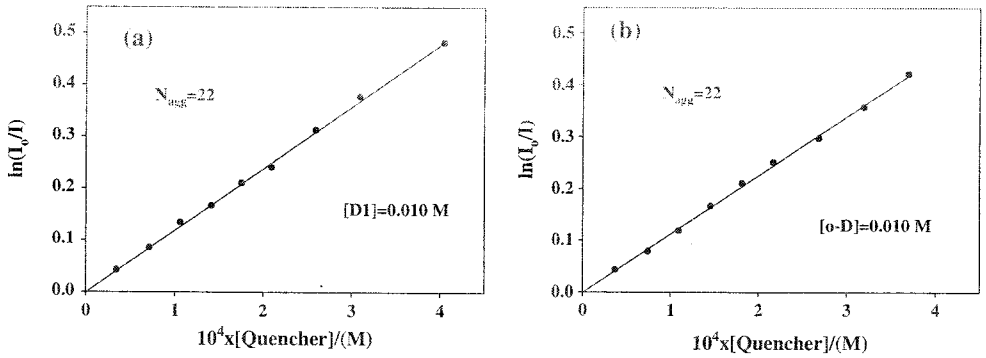

Fig. 3. Influence of the quencher (cetylpyridinium chloride, CpyCl) concentration on the intensity of pyrene fluorescence in aqueous micellar solutions. (a) D1 and (b) o-D. T = 303 K.

tions. Consequently, in order to compare the average aggregation numbers, it is necessary to estimate N_{agg} under working conditions assuring the presence of spherical micelles for all the surfactants studied. The N_{agg} values obtained are listed in Table 1. The average aggregation numbers corresponding to the surfactant pair bearing a xylidine spacer, o-D and m-D, are close to those obtained for the same surfactants by Wattebled et al. using time-resolved fluorescence quenching measurements, TRFQ, at room temperature [48]. For the surfactant pair D1 and D2, bearing a butylidene spacer, the values of N_{agg} estimated in this work are somewhat smaller than those obtained in Ref. [46]. The N_{agg} values listed in Table 1 are similar to those found by Danino et al. using TRFQ measurements at 298 K [49] for dodecyl-α,ω-bis(alkyltrimethylammonium bromide) dimeric surfactants, 12-s-12,2Br$^-$, having flexible spacers.

12-s-12,2Br$^-$ surfactants show morphological transitions when surfactant concentration increases [50]. The surfactant concentration above which the morphological transition from spherical micelles into elongated ones occurs is usually called "the second cmc" (C') [51]. The origin of C' is related to the fact that elongated micelles with moderate aggregation numbers are energetically disfavored [51]. For the dimeric surfactants used in this work, C' values were determined by using the method developed by Kuwamoto et al. [36]. SPQ is a zwitterionic inner salt highly soluble in water, which remains in the aqueous bulk phase without trapping in the cationic micelles. The SPQ emission fluorescence is quenched by halide ions via a collisional mechanism. Fig. 4 shows the Stern–Volmer plots for the quenching of SPQ fluorescence by the m-D surfactant in pure water at low as well as at high surfactant concentrations. The observed quenching can be ascribed to the

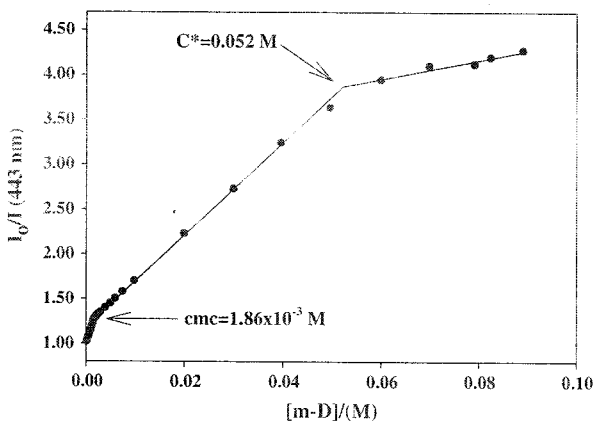

Fig. 4. SPQ fluorescence quenching in aqueous m-D micellar solutions. T = 303 K.

free chloride ions dissociated from the surfactant. Fig. 4 shows two distinct breaks, the first giving the cmc and the second giving C'. The first variation in the Stern–Volmer plot slope can be attributed to the counterion binding of micelles. The second could be assigned to a decrease in the micellar ionization degree accompanying the transition from spherical to elongated micelles. The second cmc values are listed in Table 1.

Changes in the size and shape of micelles can also be made evident by studying an adequate chemical process. The reaction between methyl 4-nitronenzenesulfonate, MBS, and a nucleophile, such as the chloride ion, has been shown to be useful for examining the formation of elongated micelles [52,53]. Fig. 5 shows the dependence of k_{obs} for the process MBS + Cl$^-$ on surfactant concentration in D1 and m-D aqueous micellar solutions. Kinetic data for the same reaction in dodecyltrimethylammonium chloride, DTAC, are also included in Fig. 5 for the sake of comparison. The chloride ions present in the micellar reaction media come uniquely from the surfactant molecules. Since the organic substrate, MBS, as well as the chloride ions are distributed between the aqueous and micellar pseudophases, the reaction occurs simultaneously in both pseudophases. An increase in surfactant concentration results in a further incorporation of the organic substrate into the micelles. As a consequence, the contribution of the reaction taking place at the micellar interface augments and because the bromide ion concentration is much higher at the micellar surface than in the aqueous phase, the observed rate constant increases. k_{obs} is expected to reach a constant value at high surfactant concentrations for which the MBS molecules are fully bound to the micelles. This behavior is observed for surfactants with no tendency to micellar growth such as dodecyltrimethylammonium chloride, DTAC (see plot c) in Fig. 5) [54]. However, plots (a) and (b) in Fig. 5 shows that for D1 and m-D micellar solutions no plateau is found at high surfactant concentrations and the observed rate constant steadily increases upon augmenting [surfactant]. The same dependence of k_{obs} on [surfactant] was found in D2 and o-D micellar solutions. Similar trends were previously observed for the reaction MBS + Br$^-$ in 12-s-12,2Br$^-$ aqueous micellar solutions, with s = 3, 4, 5 and 6 [52,53], and for the process methyl naphthalene-3-sulfonate + Br$^-$ in 12-s-12,2Br$^-$ aqueous micellar solutions, with s = 3, 4, 5, 6, 8, 10 and 12 [54]. This kinetic behavior was explained by considering that micellar growth is accompanied, among other effects, by a diminution in the micellar ionization degree [36,50], which results in an increment in the interfacial bromide ions concentration, and thus in k_{obs}. There are other changes following the morphological transition, such as a diminution in the polarity and water content of the interfacial region, which can also influence k_{obs}. Nonetheless, the dependence of k_{obs} on [surfactant] shown in Fig. 5 can be taken as indicative of morphological transitions.

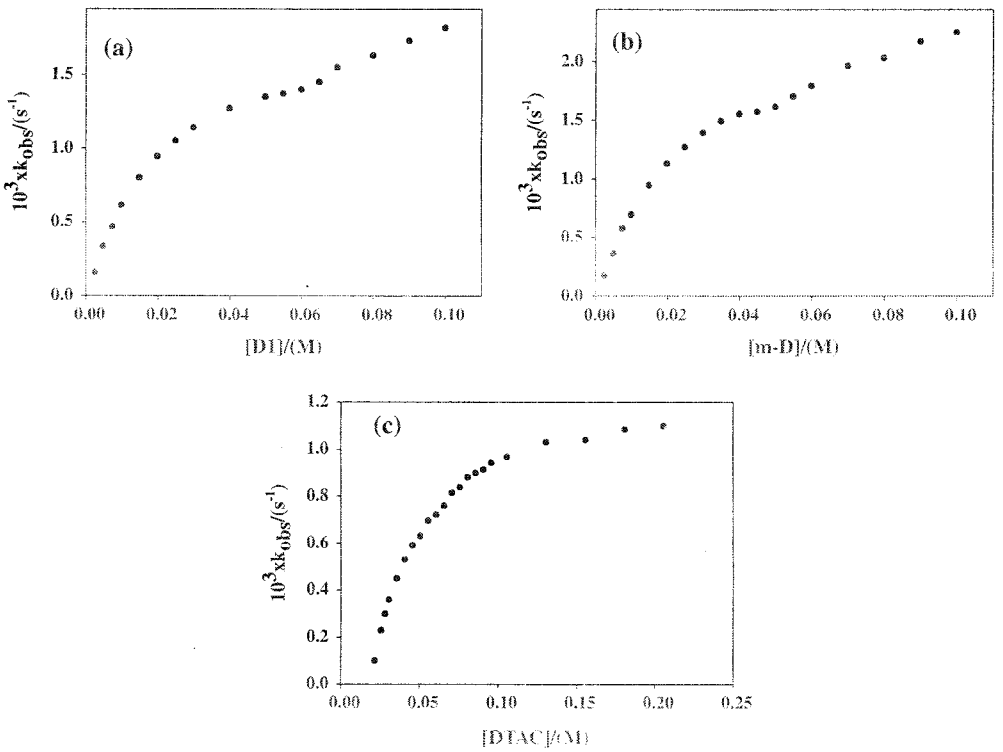

Fig. 5. Dependence of the observed rate constant, k_{obs}, for the reaction MBS + Cl⁻ on surfactant concentration at 303 K. (a) D1; (b) m-D; and (c) DTAC.

In the case of the 12-s-12,2Br⁻ dimeric surfactants a correlation between C^* and the spacer length was found for $2 \leqslant s \leqslant 5$ [50], the second cmc being higher the longer the spacer length is. Camesano and Nagarajan [55] explained this result by considering that in the case of cationic dimeric surfactants there are two Gibbs energy terms which mainly control the size and shape of the micelles that will form: the repulsive electrostatic interactions between head groups and the extra packing contribution to the deformation of the surfactant tails. The latter considers the packing constraints on the tails, as they are connected by the spacer, in order to pack within the micelle core, meeting liquid-like density constraints. Both energetic terms favor the micellar growth more the shorter the spacer length is. For the surfactants studied, the calculated maximum length of the spacers are 3.87 Å, 2.56 Å, 2.92 Å, and 5.05 Å for D1, D2, o-D, and m-D, respectively [55]. As expected we found $C^*(D1) > C^*(D2)$ and $C^*(m\text{-}D) > C^*(o\text{-}m)$. However, $C^*(o\text{-}D)$ should be higher than $C^*(D2)$, whereas the experimental results show the opposite trend. In order to rationalize the experimental data, the packing parameter, $P = v/a_o l_c$, will be considered [56]. This factor was used in order to explain the behavior of the micellar morphology, the sphere to rod transitions for example, with the length (l_c) and volume (v) of the tail chain of the surfactant, and the optimum surface area occupied by a surfactant head group at the micelle core–bulk phase interface (a_o). A reduction in the packing parameter favors the formation of spherical micelles. The length and volume of the tail chain is similar for all the surfactants investigated. The authors assumed that the optimum head group area per surfactant molecule at the micellar surface, a_o, can be approximately estimated by the minimum surface area per head group at the air-solution interface, A_{min}, obtained by surface tension measurements. Fig. 6 shows the dependence of the surface tension on the ln([surfactant]) for aqueous D1 solutions. The surface excess concentration, Γ_{exc}, and the minimum adsorbed area per molecule, A_{min}, have been calculated using the Gibbs equation:

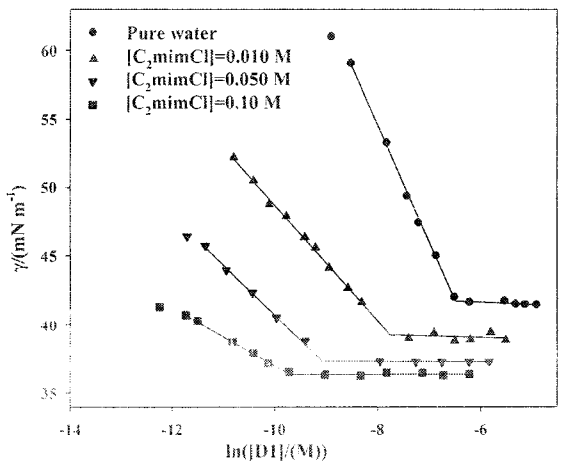

Fig. 6. Dependence of the surface tension, γ, on ln([surfactant]) in water–C_2mimCl D1 solutions. T = 303 K.

$$\Gamma_{exc} = -\frac{1}{nRT}\left(\frac{d\gamma}{d\ln[\text{surfactant}]}\right) \quad (2)$$

and the equation:

$$A_{min} = (N_A \Gamma_{exc})^{-1} \quad (3)$$

In Eqs. (2) and (3) R and T have their usual meaning, N_A is Avogadro's number and n is a constant which depends on the number of species constituting the surfactant and which are adsorbed at the interface. A value of $n = 2$ was considered for the dimeric surfactants [57]. There is controversy regarding the value of n to be used to calculate A_{min} for dimeric surfactants ($n = 2$ or $n = 3$). However, the trend of A_{min} on the spacer length is not affected by n. There

are some limitations in the use of Eq. (2), pointed out by Thomas et al. and Eastoe et al. [58–61], but this would not affect the qualitative discussion of the A_{min} values. These values are 104 Å^2, 97 Å^2, 94 Å^2, and 98 Å^2 for D1, D2, o-D, and m-D, respectively. On these basis one would expect that C^*(D1) > C^*(D2) ~ C^*(m-D) > C^*(o-D), in agreement with the observations. The small A_{min} values experimentally found for o-D and m-D can be explained by considering that the phenyl ring of the dimeric surfactant molecules is buried toward the micelle interior, with the cationic ammonia groups protruding into the aqueous phase, as is shown by the ROESY experiments.

The fluorescence maximum, λ_{max}, of the probe pyrene-3-carboxaldehyde, P3C, in micellar solutions could provide a direct measure of the polarity of the micelle-bulk interfacial region [35]. The fluorescence emission spectra of P3C were recorded at [surfactant$_m$] = 0.01 M. It was found that the emission spectra were complex, being the result of the sum of those corresponding to the P3C molecules localized in the aqueous phase and in the micellar interfacial region. In order to resolve the two contributions to the total fluorescence emission intensity, a deconvolution software was used [62]. The fluorescence emission spectrum of P3C in water, in the absence of surfactant, was also recorded in order to get the λ_{max}(water) value to be used in the curve-fitting deconvolution. Fig. 2S (Supplementary Material) shows the result of the deconvolution in aqueous D1 micellar solutions. The λ_{max} values were 445 ± 1 nm, 445 ± 1 nm, 443 ± 1 nm, and 443 ± 1 nm for D1, D2, o-D, and m-D, respectively. Taking the experimental errors into account, these data indicate that the polarity of the interfacial region of all the dimeric micelles investigated is similar.

3.2. Micellization of cationic dimeric surfactants in water–ionic liquid solutions

The aggregation of the dimeric surfactants in water–ionic liquid solutions, at several IL concentrations, was studied by surface tension measurements. Fig. 6 shows the results obtained in water–C_2mimCl D1 solutions. One can see in this figure that an increment in the IL concentration leads to a reduction in the cmc, for [IL] up to 0.10 M. A similar trend was found for all the dimeric surfactants investigated in water–C_4mimCl and water–C_6mimCl solutions. Table 2 summarizes the experimental cmc values. For IL concentrations higher than 0.10 M the surface tension variation within the surfactant concentration range below the cmc is too small and the errors affecting the estimated cmc values too high. With this in mind the cmc's corresponding to [IL] ⩾ 0.10 M were obtained by using a fluorescent method, based on the variations of the pyrene intensity ratio I_I/I_{III} following the micellization process. All I_I/I_{III} plots show a decrease as the total surfactant concentration increases, associated with the formation of micelles (see Fig. 3S, Supplementary Material). In order to calculate the cmc values, the procedure proposed by Zana et al. was used [63]. I_I/I_{III} experimental data were fitted to a sigmoid (Boltzmann type) curve, and the center of the sigmoid was identified as the cmc. These data are also summarized in Table 2. The experimental data clearly show that for 0 < [IL] ⩽ 0.10 M an increase in the IL concentration causes a reduction in the cmc, similarly to typical background electrolytes such as NaCl. However, for 0.10 M < [IL] ⩽ 0.50 M the cmc increases when the IL concentration augments. A similar dual effect of the IL concentration on the cmc of conventional surfactants has been previously found [27,64]. However, in other cases only an increase in the cmc of the surfactants when the IL concentration increases was found [65]. More complex variations of the cmc of surfactants upon changing [IL] were also observed [29], which were rationalized by considering the ILs as co-surfactants.

An IL added to an aqueous surfactant solution could have three different roles: as a background electrolyte, as a polar organic solvent, and as a co-surfactant. In regard to the latter, no critical micelle concentration was detected for C_2mimCl and C_4mimCl [30]. For C_6mimCl a cmc close to 0.90 M was proposed from surface tension measurements [30], although no micellization was found by conductivity measurements [30]. The rather short alkyl chain and the hydrophilicity of the chloride counterion do not favor micellization. Therefore, the use of the imidazolium chloride ILs with ethyl, butyl and hexyl substituents should minimize their role as co-surfactant. Nonetheless, in order to further investigate if the IL molecules form mixed micelles with the dimeric surfactants, two-dimensional, 2D, rotating frame nuclear Overhauser effect spectroscopy (ROESY) was used. No cross-peaks corresponding to the interaction between surfactant protons and IL protons were observed, thus indicating that the role of the investigated hydrophilic ILs as co-surfactants is negligible under the working conditions.

Table 2
Values of the critical micellar concentration, cmc, obtained by surface tension measurements in water–IL and water–NaCl surfactant solutions. T = 303 K.

[Additive] (M)	10^3 × cmc (M)			
	D1	D2	o-D	m-D
C_2mimCl				
0.00	1.8	1.9	1.6	1.6
0.0050	0.94	0.93	0.40	0.49
0.010	0.45	0.49	–	–
0.020	0.27	–	0.16	0.20
0.050	0.10	0.098	–	–
0.10	0.082/0.087[a]	0.054	0.043/0.048[a]	0.046
0.30	0.12[a]	–	0.14[a]	–
0.50	0.17[a]	–	0.18[a]	–
C_4mimCl				
0.0050	1.0	1.2	0.45	0.47
0.010	0.77	–	–	–
0.020	0.37	0.39	0.22	0.25
0.050	0.093	–	–	–
0.10	0.097/0.10[a]	0.065	0.056/0.057[a]	0.059
0.30	0.18[a]	–	0.16[a]	–
0.50	0.27[a]	–	0.35[a]	–
C_6mimCl				
0.0050	1.2	1.5	0.57	0.64
0.010	0.89	0.92	–	–
0.020	0.42	0.44	0.33	0.35
0.050	0.15	0.17	–	–
0.10	0.11/0.13[a]	0.12	0.093/0.10[a]	0.097
0.30	0.20[a]	–	0.25[a]	–
0.50	0.47[a]	–	0.58[a]	–
NaCl				
0.0050	0.94	1.1	0.40	0.43
0.020	0.24	0.25	0.14	0.17
0.050	0.10	–	–	–
0.10	0.047/0.051[a]	0.049	0.036/0.037[a]	0.039
0.30	0.021[a]	–	0.021[a]	–
0.50	0.016[a]	–	0.014[a]	–

[a] Values estimated by using pyrene.

The influence of background electrolytes on the cmc was investigated by surface tension measurements. Table 2 summarizes the cmc values corresponding to the dimeric surfactants studied in the presence of several NaCl concentrations. For the sake of comparison, for [IL] ⩾ 0.10 M the cmc values were determined by using the pyrene fluorescence method. One can see that an increase in [NaCl] causes a reduction in the cmc for all the surfactants investigated, in the whole NaCl concentration range studied. This is an expected result since the presence of NaCl in the aqueous solution diminishes the electrostatic repulsions between the positively charged surfactant head groups within the micelles, thus favoring the aggregation process [55].

The influence of polar organic solvents on the cmc of the dimeric surfactants was investigated by studying their aggregation process in water–ethylene glycol and in water–formamide binary

mixtures. These two solvents do not incorporate into the micellar aggregates, but mainly remain in the bulk phase. The experimental data are summarized in Table 3. Ethylene glycol has a permittivity lower than water and formamide has a permittivity higher than water [66]. However, in both cases an increase in the amount of organic solvent causes an increment in the cmc. This cmc increase has been found for several water–organic solvent mixtures (with organic solvents which preferentially remain in the bulk phase) characterized by permittivities higher as well as lower than that of pure water [67]. Speaking in general, the addition of an organic solvent renders the bulk phase a better solvent for the surfactant molecules. This would make the transfer of the hydrophobic tail from the bulk phase into the micelles less favorable and, as a consequence, the Gibbs energy term, ΔG^{o}_{trans}, increases (becomes less negative), making ΔG^{o}_{M} less negative.

For all the water–IL solutions studied, a diminution in the cmc is observed when the [IL] increases up to 0.10 M. The cmc values, within the range $0 < [IL] \leqslant 0.10$ M, follow the trend cmc(C_2mimCl) < cmc(C_4mimCl) < cmc(C_6mimCl). This trend also holds for [IL] higher than 0.10 M, although within this IL concentration range the cmc augments when the ionic liquid concentration increases. Taking the effect of [NaCl] and [polar organic solvent] on the cmc into account, the data in Table 2 could be explained by considering that the hydrophilic ionic liquids investigated behave simultaneously as a background electrolyte and as a polar organic solvent. The extent of the contributions of one or the other role depends on the IL concentration as well as on the IL hydrophobicity. An increase either in the IL concentration or in the IL alkyl chain length favors the role of the ionic liquid as a polar organic solvent.

The water–IL surfactant solutions were further investigated by using dynamic light scattering measurements, DLS, which permit the estimation of the average hydrodynamic diameter of the micellar aggregates. Fig. 7 shows the dependence of the average hydrodynamic diameter of D2 and o-D on the ionic liquid concentration. The values of this magnitude for the D1 and m-D aggregates in water–IL binary mixtures are listed in Table S1, together with the plot of %Intensity(number) against the diameter for the water–IL o-D micellar solutions (Fig. 4S, Supplementary Material). For IL concentrations higher than 0.5 M the solutions turned opaque. Some measurements were done for D1 and m-D surfactants, the results being similar to those of D2 and o-D, respectively. Fig. 7 shows that an increase in the ionic liquid concentration results in an increase in the size of the micelles of the dimeric surfactants except for C_6mimCl. In the latter case the micelle size remains nearly constant for $[C_6mimCl] \geqslant 0.10$ M. The hydrodynamic radius increment experimentally observed follows the trend C_2mimCl > C_4mimCl > C_6mimCl.

Data in the literature show that the effect of ionic liquid addition on the micelles size depends on both the surfactant and the IL nature. Rai et al. [68] found that the average size of the micelles in aqueous solutions of the anionic dodecylbenzene sulfonate, SDBS, increases drastically upon addition of butyl-3-methylimidazolium hexafluorophosphate, C_4mimPF_6, up to ~0.15 M. This may not be unexpected, as the addition of organic ions of opposite charge to ionic dimeric surfactants may induce massive aggregation effects [69]. However, addition of butyl-3-methylimidazolium tetrafluoroborate, C_4mimBF_4, or of the inorganic salts $NaPF_6$ and $NaBF_4$ only gradually increases the aggregate size. For aqueous solutions of another anionic surfactant, sodium dodecylsulfate, SDS, the addition of C_4mimBF_4 causes a gradual increase in the micellar size [70]. Behera et al. studied the effect of C_6mimBr addition on the average size of micelles of the cationic cetyltrimethylammonium bromide up to an IL concentration close to 1.3 M [71]. Initially, they found a gradual increase in the average aggregate size from 1.2 nm to 5.1 nm, by increasing [IL] up to 0.41 M. However, a subsequent increase in the ionic liquid concentration does not affect the aggregate size, within experimental errors. Similarly, no significant changes were found in the size of micelles of the nonionic Triton X-100 in aqueous solution, when C_4mimPF_6 was added up to 2.1 wt% [72]. In contrast, the addition of C_4mimBF_4, to aqueous solutions of the zwitterionic N-dodecyl-N,N-dimethyl-3-ammonio-1-propanesulfonate, SB12, was reported to decrease the micellar size from 7.1 nm, in pure water, to 1.7 nm in the presence of [C_4mimBF_4] = 0.089 M [73]. With the goal of understanding the effect of the ionic liquids on micellar size and considering their double role as background electrolytes and as polar organic solvents, the influence of NaCl and of polar organic solvents on the micelle size will be considered next.

Fig. 7 shows that an increase in [NaCl] leads to an increase in the average hydrodynamic diameter of the dimeric micelles. As in the case of the diminution of the cmc upon increasing [NaCl], this observation can be explained by the reduction of the electrostatic repulsions between the positively charged head groups within the aggregates [55], which allows the formation of larger aggregates. Although other contributions to ΔG^{o}_{M} are also dependent on the ionic concentration [55], the electrostatic Gibbs energy term is mainly responsible for the growth of the aggregates found when salts are added to micellar solutions. The fluorescence quenching of pyrene by CpyCl was used in order to estimate the N_{agg} of the D2 micelles in the presence of the NaCl, with [surfactant] = 0.01 M. The according values of N_{agg} were 23, 26, 37, and 50 for NaCl concentrations equal to 0 M, 0.1 M, 0.3 M, and 0.5 M, respectively. That is, an increase in [NaCl] provokes an increment in the N_{agg}, as was predicted. A similar dependence of N_{agg} on [NaCl] is expected for D1, o-D, and m-D surfactants.

With regard to the effect of polar organic solvents on the micelle average aggregation number, several authors have reported that an increase in the content of the organic solvent (which remains mainly in the bulk phase) results in a decrease in N_{agg} (for conventional ionic, nonionic and zwitterionic surfactants as well as for cationic dimeric surfactants) [74,75]. This diminution of N_{agg} was rationalized by considering the variations caused in the interfacial Gibbs energy contribution, $\Delta G^{o}_{interfacial}$, to ΔG^{o}_{M} by the presence of the organic solvent. This size-dependent term takes into account that the formation of a micelle creates an interface allowing for contact between the hydrophobic core and the bulk phase (the water–organic solvent mixture). It is a large positive term, which decreases as the micelle size increases, thus favoring micellar growth [55]. $\Delta G^{o}_{interfacial}$ is proportional to the hydrophobic core-bulk phase interfacial tension. It is reasonable to expect that the variations in the hydrophobic core/bulk phase interfacial tension are proportional to the changes in the air/bulk phase surface tension, γ, when an organic solvent is added [76]. This surface tension decreases upon increasing the polar organic solvent content [76], making $\Delta G^{o}_{interfacial}$ less positive and favoring smaller micelles in the water–organic solvent mixtures than in water. The lower the surface tension of the water–organic polar solvent mixture, the smaller the average aggregation number is. The N_{agg} values of D2 and m-D were estimated via

Table 3
Values of the critical micellar concentration, cmc, in water–polar organic solvent dimeric surfactant solutions at 303 K.

Water–ethylene glycol	$10^3 \times$ cmc (M)			
	D1	D2	o-D	m-D
20 wt%	2.4	2.3	2.0	2.1
50 wt%	7.5	7.4	7.1	7.3
Water–formamide				
10 wt%	3.2	3.0	2.3	2.5
20 wt%	4.7	4.5	3.7	3.9

wt%: Percentage of organic solvent by weight.

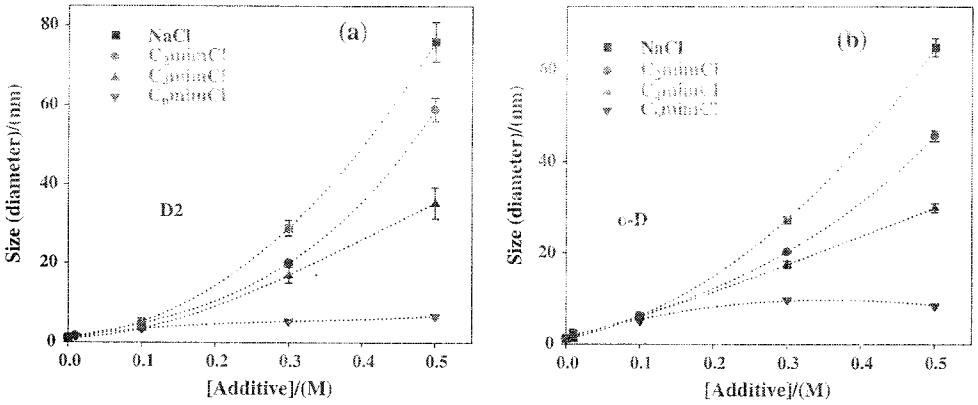

Fig. 7. Average hydrodynamic diameter of the micelles estimated by DLS measurements in aqueous surfactant solutions in the presence of different additives. [Surfactant] = 0.05 M and T = 303 K. (a) D2 and (b) o-D.

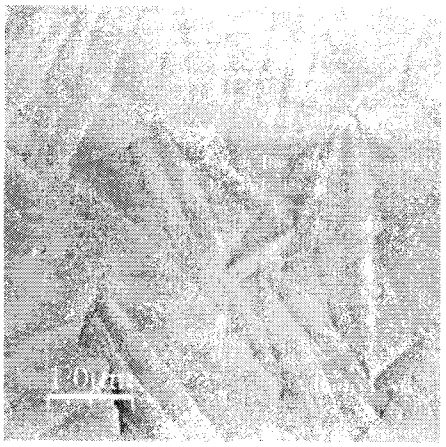

Fig. 8. AFM topographic image of aqueous C4mimCl 0.05 M adsorbed at a mica surface.

the fluorescence quenching of pyrene by CpyCl, with [surfactant] = 0.01 M, in water–ethylene glycol with 20% by weight of organic solvent. The results were 20 and 19 for D1 and m-D, respectively. That is, N_{agg} decreases when a polar organic solvent is added to the micellar solution. A similar result was expected for the D1 and o-D surfactants.

The influence of the ionic liquids on N_{agg} was also studied using the fluorescence quenching of pyrene by CpyCl. For D2, with [D2] = 0.01 M and [IL] = 0.5 M, the average aggregation number estimated was 44, 39 and 33 for added C_2mimCl, C_4mimCl, and C_6mimCl, respectively. That is, for [IL] = 0.5 M, $N_{agg}(C_2mimCl) > N_{agg}(C_4mimCl) > N_{agg}(C_6mimCl)$, in agreement with the trend shown in Fig. 7 for the average hydrodynamic radius.

From the above results it is possible to conclude that the variation in the micellar size caused by the ionic liquid addition to the aqueous micellar solution is the result of two effects operating in opposite directions. On one hand, an increase in the ionic liquid concentration leads to an increment in the ionic strength of the bulk phase (background electrolyte effect). As a consequence, the electrostatic repulsions at the micellar interface diminish, favoring the formation of larger aggregates. On the other hand, the presence of the IL in the bulk phase decreases the hydrocarbon core-bulk phase interfacial tension, making the interfacial Gibbs energy contribution less positive (polar organic solvent effect). This renders the formation of smaller micelles more favorable. The diminution of the air/bulk phase (water–IL solution) surface tension caused by the presence of the ionic liquid follows the trend $\gamma(C_2mimCl) < \gamma(C_4mimCl) < \gamma(C_6mimCl)$ [27]. Therefore, the reduction in the micellar size provoked by the ionic liquids is expected to be larger the longer the alkyl chain of the IL is. The experimentally observed micellar size variations caused by the ILs addition are accordingly the result of the ionic liquids dual role as background electrolytes and as organic polar solvents.

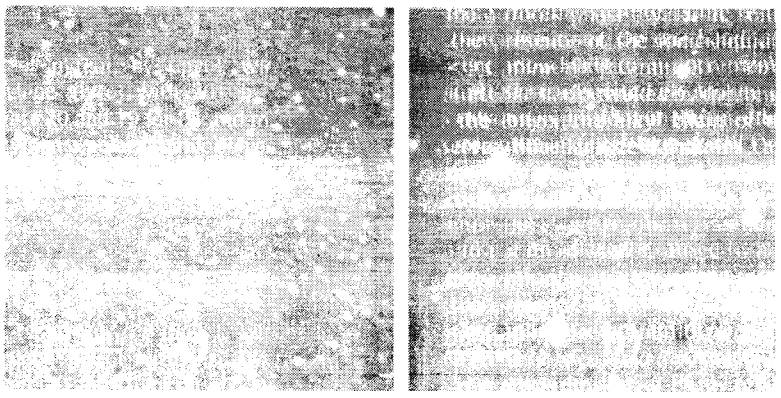

Fig. 9. AFM topographic image of IL–surfactant solutions adsorbed at a mica surface. (a) Aqueous D1 micellar solutions with [D1] = 0.05 M. (b) Water–C_4mimCl D1 micellar solutions with [C_4mimCl] = 0.5 M and [D1] = 0.05 M.

Structural information can be extracted from Atomic Force Microscopy, AFM, images. With this in mind, AFM experiments were carried out in order to get information about the changes caused by the increase in IL concentration in the micellar solutions. In double-distilled water the mica surface is negatively charged, so that the positively charged micelles, as well as the surfactant monomers and the cations of the ionic liquids, adsorbed readily. The surfactant concentration used was 0.05 M, similar to that present in the DLS measurements. The authors found experimental problems related to the precipitation and/or crystallization of the ionic liquids on the mica surface during the drying process. This was particularly notable for C_2mimCl (see Fig. [illegible]). Some AFM images corresponding to water–C_4mimCl binary mixtures could be obtained (see Fig. 9). In [illegible] spherical micelles are observed together with monomers or clusters of monomers adsorbed at the mica surface. The micelle size distribution is about 1.2–2.0 nm, in agreement with the DLS data in bulk solution. This image is analogous to those obtained by other authors for micelles adsorbed at surfaces by using AFM [78]. Fig. 9(b) shows micelles, with a wide size distribution between 12 and 28 nm, as well as surfactants monomers adsorbed at the mica surface. These micelles are clearly larger than those observed in the absence of IL. Fig. 9a and b seem to indicate that the addition of this IL causes a substantial increase in the dimeric micelle size, in agreement with fluorescence and DLS measurements. Nonetheless, care has to be taken when reaching for conclusions from the AFM images due to the precipitation of the ionic liquids on the mica and the fact that the species adsorbed at the surface could be different from those in solution.

4. Conclusions

The micellization process of four cationic dimeric surfactants, with dodecyl chains and comprising rigid spacer groups, has been studied in water–ionic liquid solutions. The ionic liquids investigated were ethyl-, butyl-, and hexyl-3-methylimidazolium chlorides, C_2mimCl, C_4mimCl, and C_6mimCl, respectively. For a better understanding of the systems studied, the micellization process was also investigated in aqueous NaCl solutions, in water–ethylene glycol and in water–formamide binary mixtures. It was found that the Gibbs energy of micellization in water is similar for all the dimeric surfactants investigated. This points out that – within the range of variations made – the different nature of the butylidene and xylidine spacers hardly influences the self-organization process. The surfactants studied undergo morphological transitions from spherical to elongated micelles in water upon augmenting surfactant concentration. The tendency to form elongated micelles increases when the area per surfactant molecule at the micelle interface, a_0, decreases. For the two dimeric surfactants with xylidine spacers, ROESY experiments show that part of the spacer is buried towards the micelle interior and, as a consequence, they show a stronger tendency to micellar growth than was expected on the basis of their spacers' length. This is an important topic because micellar growth improves the micelle solubilization capacity of water-insoluble species [79], relevant for many surfactant applications. It also affects properties of surfactant solutions such as their rheological behavior and their foamability [80,81].

The addition of the ionic liquids to the aqueous surfactant solutions leads initially to a diminution of the cmc for IL concentrations up to 0.10 M. For higher ionic liquid concentrations, an increase in [IL] results in an increase of the cmc. The observed minima in the cmc are explained by considering that the investigated ILs play a double role, namely as background electrolytes and as polar organic solvents. When the role of the ionic liquids as background electrolyte dominates, an [illegible] increment in the ionic strength and [illegible] between the cationic head groups in the micelle interface diminishes. As a consequence the cmc decreases. On the other hand, when the ionic liquids mainly act as polar organic solvents, an increase in the amount of IL makes the bulk phase a better solvent for the hydrophobic chains of the surfactants. Thus the Gibbs energy for the transfer of the surfactant tails from the bulk phase into the micellar interior will be less negative, making the micellization process more difficult and, therefore, increasing the cmc. The relative contribution as a polar organic solvent increases when the IL concentration augments. It also increases with the length of the ionic liquid's alkyl chain.

An increment in the ionic liquid concentration causes an increase in the average hydrodynamic diameter, d, of the aggregates [illegible] within the whole IL concentration range. Contrary to the case of C_6mimCl, the micelle size remains nearly constant at high IL concentrations. These changes can also be explained by the double role played by the ILs investigated. When the ionic liquids behave as background electrolytes, the increase in the ionic strength accompanying an increment in [IL] provokes a diminution of the electrostatic repulsions between the positively charged ionic heads within the interfacial region, favoring the formation of larger aggregates. When the ionic liquids behave as polar organic solvents, an increment in [IL] is followed by a decrease in the hydrocarbon core-bulk phase interfacial tension, this making the interfacial Gibbs energy less positive and favoring the formation of smaller aggregates. The experimental trend shown by d is the result of these two opposite effects working simultaneously.

The results obtained in this work show that addition of ILs to aqueous surfactant solutions could be used in order to tune the physicochemical properties of micelles, which could be useful for several surfactant technological applications [70]. For instance, the increase in micelle size caused by the addition of ILs could improve the solubilization capacity of the dimeric micelles, which plays an important role in many technological and biotechnological processes [illegible]. The micelle solubilization capacity is also of increasing importance in separation science, for example, in micellar-enhanced ultrafiltration, micellar extraction, micellar liquid chromatography, and micellar electrokinetic capillary chromatography [83].

Acknowledgments

This work was financed by the DGCYT (Grant BQU2009-07478), the FEDER funds, and Consejería de Innovación, Ciencia y Empresa de la Junta de Andalucía (FQM-274 and P12-FQM-1105). The authors want to thank Dr. Consuelo Cerrillos for her help in the AFM measurements.

Appendix A. Supplementary data

Supplementary data associated with this article can be found, in the online version, at http://dx.doi.org/10.1016/j.jcis.2014.05.064.

References

[1] F.M. Menger, J.S. Keiper, Angew. Chem., Int. Ed. 39 (2000) 1906–1920.
[2] R. Zana, Adv. Colloid Interface Sci. 97 (2002) 205–253.
[3] R. Zana, J. Xia (Eds.), Gemini Surfactant Synthesis, Interfacial and Solution Phase Behavior and Applications, M. Dekker Inc., New York, 2004.
[4] [illegible], P. Di Profio, A. Fontana, Langmuir 30 (2014) 2979–2987.
[5] [illegible] Dong, X. [illegible] S. Mao, Y. Du, M. Liu, Colloid Polym. Sci. 292 (2014) [illegible].
[6] [illegible] Chem. Eur. Chem. 16 (2010) 4686–4692.
[7] [illegible] Energy Fuels 25 (2011) 162–171.
[8] [illegible] R.J.M. Nolte, O. Soderman [illegible] P. Garidel, A. Kremer, C. [illegible]

McGregor, C. Perrin, G. Ronsin, [illegible] Angew. Chem. Int. Ed. 42 (2003) 1448–1457.
[9] V. Sharma, M. Borse, S. Johari, K.B. Pal, S. Devi, Tenside Surfactants, Deterg. 3 (2005) 163–167.
[10] C. Borde, V. Nardello, L. Wattebled, [illegible] J. Phys. Org. Chem. 21 (2008) 652–658.
[11] L. Leclercq, A.R. Schmitzer, [illegible]
[12] N. Noujeim, L. Leclercq, [illegible]
[13] Ch. Tanford, The Hydrophobic [illegible] New York, 1980.
[14] Y. Moroi, Micelles: Theoretical and Applied Aspects, [illegible] New York, 1992.
[15] T. Welton, Chem. Rev. 99 (1999) [illegible]
[16] A. Kokorin (Ed.), Ionic Liquids: [illegible] Properties, New Approaches, InTech, 2011.
[17] G. Liu, R. Zhong, R. Hu, F. Zhang, Biophys. Rev. Lett. 7 (2012) 121–134.
[18] D.D. Patel, J.M. Lee, Chem. Rec. 12 (2012) 329–[illegible].
[19] G.A. Baker, S.N. Baker, S. Pandey, F.V. Bright, Analyst 130 (2005) 800–808.
[20] K.Y. Yung, A.J. Schadok-Hewitt, N.P. Hunter, F.V. Bright, G.A. Baker, Chem. Commun. 47 (2011) 4665–4777.
[21] O. Cabeza, S. García-Garabel, L. Segade, M. Domínguez-Pérez, E. Rilo, L.M. Varela, in: A. Kokorin (Ed.), Ionic Liquids: Theory, Properties, New Approaches, InTech, 2011, pp. 114–136 (Chapter 5).
[22] J. Ködderman, C. Wertz, A. Heintz, R. Ludwig, Angew. Chem., Int. Ed. 45 (2006) 3697–3702.
[23] I. Khan, K.A. Kurnia, F. Mutelet, S.P. Pinho, J.A.P. Coutinho, J. Phys. Chem. B 118 (2014) 1848–1860.
[24] G. Luo, X. Qi, Ch. Han, Ch. Liu, [illegible] 531–[illegible].
[25] A. Pan, S.S. Mati, B. Naskar, [illegible] J. Phys. Chem. B 117 (2013) 7578–7592.
[26] A.K. Tiwari, [illegible] Sonu, S.K. Saha, [illegible]
[27] Y. Shang, T. Wang, X. Han, [illegible] 8852–8857.
[28] X. Wang, R. Wang, Y. Zheng, [illegible] J. Phys. Chem. B 117 (2013) 1886–1895.
[29] F. Comelles, I. Ribera, J.J. Gon[illegible] (2012) 14522–14530.
[30] J. Luczak, J. Hupka, J. Thoming, C. Jungnickel, Colloids Surf. A 329 (2008) 125–133.
[31] A. Laschewsky, K. Lunkenheimer, R.V. Rakotoaly, L. Wattebled, Colloid Polym. Sci. 283 (2005) 469–479.
[32] P.P. Acharya, H. Kunieda, in: P. Somasundaran (Ed.), Encyclopedia of Colloid and Surface Science, second ed., CRC Press, Boca Raton, FL, 2006, p. 6635.
[33] V.I. Martín, A. Rodríguez, M.M. Graciani, I. Robina, A. Carmona, M.L. Moyá, J. Colloid Interface Sci. 363 (2011) 284–29[illegible].
[34] R. Zana, J. Phys. Chem. B 103 (1999) pp. 1917–1922.
[35] K. Kalyanasundaram, J.K. Thomas, J. Chem. Phys. 81 (1977) 2176–2180.
[36] K. Kuwamoto, T. Asakawa, A. Ohta, S. Miyagishi, Langmuir 21 (2005) 7691–7695.
[37] M. Tachiya, Chem. Phys. Lett. [illegible]
[38] P.P. Infelta, Chem. Phys. Lett. 61 (1979) [illegible]
[39] M. Deleu, M. Paquet, C. Blecker, in: A. Hubbard (Ed.), Encyclopedia of Surface and Colloid Science, Dekker, [illegible]
[40] D.H. Wu, A.D. Chen, C.S. Johnson, [illegible]
[41] G. Fernández, A. Rodríguez, [illegible] Kinet. 35 (2003) 45–51.
[42] C. Bonan, R. Germani, P.P. [illegible] J. Phys. Chem. 54 (1990) 5331–5336.
[43] I. Horcas, R. Fernández, J.M. Gómez-Rodríguez, J. Colchero, J. Gómez-Herrero, A.M. Baro, Rev. Sci. Instrum. 78 (2007) [illegible]
[44] P. Carpena, J. Aguiar, P. Bernaola-Galván, C. Carnero Ruiz, Langmuir 18 (2002) 6054–6058.
[45] [illegible] Langmuir [illegible] (1996) 4044–4045.
[46] [illegible] Langmuir 16 (2000) 5242–5251.
[47] O. Söderman, P. Stilbs, W.S. Price, Concepts Magn. Reson. 231 (2004) 121–135.
[48] L. Wattebled, A. Laschewsky, A. Moussa, J.L. Habib-Jiwan, Langmuir 22 (2006) [illegible]
[49] [illegible] (1995) 1443–1458.
[50] [illegible] Robina, M.L. Moyá, J. Phys. Chem. B [illegible]
[51] [illegible] Chem. 88 (1984) 5713–5720.
[52] [illegible] J. Colloid Interface Sci. 328 (2008) [illegible]
[53] [illegible] M.L. Moyá, J. Phys. Chem. B 113 (2009) [illegible]
[54] [illegible] C. Fernández, M.L. Moyá, Langmuir 26 [illegible]
[55] [illegible] Colloids Surf., A 167 (2000) 165–177.
[56] J. Mitchell, B. Ninham, J. Chem. Soc., Faraday Trans. 2 (77) (1981) 601–629.
[57] T.W. Kassem, A.A. El-Sawy, A.S. Mohamed, A.E. Mohamed, F.M. Abdelhafiz, Tenside Surfactants Deterg. [illegible] 277–282.
[58] J.R. Lu, E.A. Simister, E.M. Lee, R.K. Thomas, Langmuir 8 (1992) 1837–1844.
[59] Z.X. Li, J.R. Lu, R.K. Thomas, Langmuir 13 (1997) 3681–3685.
[60] A.D. Downer, J. Eastoe, A.R. Pitt, J. Penfold, R.K. Heenan, Colloids Surf., A 156 (1999) [illegible]
[61] J. Eastoe, S. Nave, A. Downer, A. Paul, A. Rankin, K. Tribe, Langmuir 16 (2000) [illegible]
[62] [illegible] M. García-Blanco, M. Blázquez, Comput. Chem. 13 [illegible]
[63] [illegible] (1997) 229–232.
[64] [illegible] Moulik, J. Phys. Chem. B 117 [illegible]
[65] [illegible]
[66] [illegible] second ed., Verlag Chemie, [illegible]
[67] [illegible] Langmuir 24 (2008) 12785–12792.
[68] [illegible] S. Pandey, Langmuir 26 [illegible]
[69] [illegible] Langmuir 23 (2007) 10044–10052.
[70] [illegible] S. Pandey, Langmuir [illegible] (2007) 13307–13315.
[71] [illegible] S. Pandey, J. Phys. Chem. B 113 (2009) 786–793.
[72] [illegible] S. Pandey, J. Colloid Interface Sci. 307 (2007) 235–245.
[73] [illegible] Langmuir 24 (2008) 6462–6469.
[74] [illegible] G. Fernández, J. Colloid Interface Sci. 316 (2007) 787–795.
[75] A. Rodríguez, M.M. Graciani, M. Angulo, M.L. Moyá, Langmuir 23 (2007) [illegible]
[76] D. Khossravi, K.A. Connors, J. Solution Chem. 22 (1993) 677–694, and references therein.
[77] W. Liu, [illegible] H. Wang, [illegible] J. Chem. Eng. Data 140 (2011) 68–[illegible]
[78] [illegible] Langmuir 24 (2008) 14183–[illegible]
[79] [illegible] (2006) 749–754.
[80] [illegible] J. Phys. Chem. B 104 (2000) [illegible] [illegible] Chem. B 112 (2008) 2909.
[81] [illegible] J.J. Ortega-Calvo, M.L. Moyá, [illegible]
[82] [illegible] J. Hupka, J. Phys. Chem. B 117 (2013) [illegible]
[83] [illegible] Rajagopalan, Principles of Colloid and Surface Chemistry, Marcel Dekker Inc., New York, [illegible] pp. 375–385.